Bioorganic & Medicinal Chemistry Letters xxx (xxxx) xxx–xxx

Contents lists available at ScienceDirect

Bioorganic & Medicinal Chemistry Letters

journal homepage: www.elsevier.com/locate/bmcl

Discovery of a novel 2-(1*H*-pyrazolo[3,4-*b*]pyridin-1-yl)thiazole derivative as an EP_1 receptor antagonist and *in vivo* studies in a bone fracture model

Masakazu Atobe[a,*], Kenji Naganuma[a], Masashi Kawanishi[a], Takahiko Hayashi[b], Hiroko Suzuki[c], Masahiro Nishida[b], Hirokazu Arai[b]

[a] *Laboratory for Medicinal Chemistry, Asahi Kasei Pharma Corporation, 632-1 Mifuku, Izunokuni, Shizuoka 410-221, Japan*
[b] *Laboratory for Pharmacology, Asahi Kasei Pharma Corporation, 632-1 Mifuku, Izunokuni, Shizuoka 410-221, Japan*
[c] *Laboratory for Safety Assessment & ADME, Pharmaceutical Research Center, Asahi Kasei Pharma Corporation, 632-1 Mifuku, Izunokuni, Shizuoka 410-2321, Japan*

ARTICLE INFO

Keywords:
EP_1 receptor
Prostaglandin E_2
Target validation
Oral administration
Bone fracture healing

ABSTRACT

We describe a medicinal chemistry approach to the discovery of a novel EP_1 antagonist exhibiting high potency and good pharmacokinetics. Our starting point is **1**, an EP_1 receptor antagonist that exhibits pharmacological efficacy in cystometry models following intravenous administration. Despite its good potency *in vitro*, the high lipophilicity of **1** is a concern in long-term *in vivo* studies. Further medicinal chemistry efforts identified **4** as an improved lead compound with good *in vitro* ADME profile applicable to long term *in vivo* studies. A rat fracture study was conducted with **4** for 4 weeks to validate its utility in bone fracture healing. The results suggest that this EP_1 receptor antagonist stimulates callus formation and thus **4** has potential for enhancing fracture healing.

Prostaglandin E_2 (PGE_2) is a metabolite of arachidonic acid and interacts with various important bioactive ligands to exhibit physiological functions.[1] Most of these functions involve the four prostaglandin receptors EP_1, EP_2, EP_3 and EP_4.[2] EP_1 is most abundant on the C fibers of the bladder[3] and EP_1 antagonistic activity may be useful for the treatment of overactive bladder (OAB).[4] We previously reported pyrazole/indazole derivatives which have highly potent EP_1 receptor antagonistic activity with good selectivity against EP_2-EP_4,[5–7] and their anti-OAB effect was identified using a rat cystometry model following 1 mg/kg iv administration of the most potent compound **1**.[7] However, clinical study results by Ono Pharmaceutical showed that their EP_1 receptor antagonist ONO-8539 did not meet their clinical end-point, leading them to conclude that EP_1 receptors may not be promising targets for OAB treatment.[8] And also, KRP-EPA-605, which was co-development by Kyorin and Kissei, was in phase I clinical trials for the treatment of overactive bladder. However, the studies was discontinued in 2014.[9] On the other hand, Eli-Lilly reported the generation of $EP_1^{-/-}$ KO mice as a rat-bone fracture model[10] and indicated that EP_1 receptor is a negative regulator that acts at multiple stages of the fracture healing process and that the inhibition of EP_1 signaling may enhance fracture healing. These results encouraged us to evaluate the utility of EP_1 receptor antagonists for the clinical treatment of bone fractures. However, genetic target validation studies to date have been unable to determine the interaction between KO mouse features and the effects of small molecules, in some cases. Consequently, we have conducted optimization studies of our compounds and target validation studies with our optimum small molecule.

Our compound, 2-(3-phenyl-6-(trifluoromethyl)-1*H*-indazol-1-yl) thiazole-4-carboxylic acid (**1**) (Fig. 1), exhibits high EP_1 antagonistic activity with excellent selectivity against EP_2–EP_4 and other GPCR receptors[7] but its high lipophilicity complicates pharmacokinetics upon oral administration. We therefore increased the number of sp^3 atoms or charged atoms to reduce the lipophilicity and improve the pharmacokinetics of the compound and investigated the long term effects of these derivatives in *in vivo* studies.

The structure activity relationship (SAR) results for the derivatives are summarized in Table 1. 4*H*-Hydroindazole (**2**) reduced EP_1 activity and hydro-pyrane at the 3-position of the indazole (**3**) also showed good EP_1 activity and a lower clog P. 1*H*-Pyrazolo[3,4-*b*]pyridine (**4**) exhibited the best EP_1 activity, low clog P, and good metabolic stability. Moving the nitrogen atom to the 4-position on the indazole to provide 1*H*-pyrazolo[4,3-*b*]pyridine (**5**) or the addition of a carbon at the 1-position to generate indazole (**6**) reduced EP_1 activity. We synthesized several derivatives of 1*H*-pyrazolo[3,4-*b*]pyridine (**7**–**9**) but their activities were lower than that of **4**, and thus we chose **4** as the most promising compound for evaluation in an *in vivo* pharmacokinetics study (Table 1).

The selectivity of $EP_{1–4}$ receptors of **4** is shown in Fig. 2-(a). **4** showed excellent selectivity against $EP_{2–4}$. Additionally, **4** provided a negative Ames test result. A binding panel test with **4** against other

* Corresponding author.
E-mail address: atobe.mb@om.asahi-kasei.co.jp (M. Atobe).

https://doi.org/10.1016/j.bmcl.2018.06.022
Received 13 April 2018; Received in revised form 6 June 2018; Accepted 12 June 2018

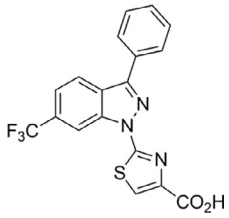

Fig. 1. 2-(3-Phenyl-6-(trifluoromethyl)-1*H*-indazol-1-yl)thia-zole-4-carboxylic acid (**1**).

GPCR and non-kinetic enzymes showed that **4** has no activity below 1 μM. The *in vitro* ADME profile of **4** is shown in Fig. 2-(b). The protein binding ability of **4** was lower than that of **1**, indicating that the physicochemical properties of **4** are superior to those of **1**. A pharmacokinetic study[11] showed that the unbound concentration of **4** was significantly higher than that of **1** and thus **4** was chosen as the most promising compound for further pharmacokinetic studies (Fig. 2-(c)).

Compound **4** was orally administered at 10 mg/kg, 30 mg/kg and 100 mg/kg and its pharmacokinetics are shown in Fig. 3. The corresponding Cmax values were 24.8 μM, 75.1 μM and 179 μM, dose-dependently (Fig. 3). Particularly, a top dose of 100 mg/kg showed to be able to expose the high concentration after 24 h. Indeed, PK study for 4 weeks was performed with doses of 30 mg/kg QD, 30 mg/kg BID and 100 mg/kg QD. The result suggest that all doses showed good exposure of **4** during 4 weeks as tool compound for long-term *in vivo* studies (Supplementary material).

A femoral fracture study[12] was performed with 30 mg/kg twice a day (BID), 30 mg/kg once a day (OD) and 100 mg/kg OD of **4** as an *in vivo* validation study of bone fracture healing. Closed femur fractures were created in 8-week-old SD mice. The most significant effect of **4** was observed in the callus area at all doses (Fig. 4-(a)): after 4 weeks administration, the callus area was significantly broader than in the vehicle control and large gaps in the bone were filled by mineralization, demonstrating that **4** stimulates the formation of callus. Photos of bone following the administration of 100 mg/kg OD are shown in Fig. 4-(b). The result was that 9 bodies out of 19 bodies showed completely cured the bone fracture (red rectangle highlighted). However, in some mice there was a delay in bone fracture healing, in contrast to $EP_1^{-/-}$ mice. Thus, EP_1 receptor antagonists may aid fracture healing but their efficacy and mechanism of action via EP_1 receptor antagonists remain unclear. Mechanistic studies are currently underway and the results will be reported in the near future.

The synthesis of compound **2** is shown in Scheme 1. Claisen condensation of **10** with benzoyl chloride was followed by $(NH_2)_2$-H_2O to give fused-pyrazole **11** in 11% yield following a literature protocol.[13] Next, Ullmann coupling with copper and amine catalyst led to *N*-arylation on the pyrazole nitrogen.[14] Finally, the hydrolysis of **12** provided **2** in 76% yield (Scheme 1).

The synthesis of compound **3** is shown in Scheme 2. The indazole cyclization via oxime ether based on a literature methodology provided the indazole **14** in 37% yield. After iodation and Boc-protection, Suzuki coupling with 2*H*-dihydro-pyran boronic acid to give the 3-2*H*-dihydropyranyl indazole in 39% yield. Finally, Ullmann type coupling with ethyl 2-bromo thiazole carboxylate and hydrolysis yielded compound **3** (Scheme 2).

The synthesis of compound **4** and **5** is shown in Scheme 3. LDA-mediated lithiation of 2-fluoro-6-trifluoromethyl pyridine **19**[15] was followed by Weinreb amide to give 3-benzoyl pyridine, and subsequently treated with $(NH_2)_2$-H_2O to give fused-pyrazole **21** in 62% yield as 2 steps. Next, Ullmann coupling led to *N*-arylation on the pyrazole nitrogen to give **22**. Finally, hydrolysis of **22** provided **4** in 90% yield. In a similar manner, the Ullmann type coupling of commercially available **23** gave **24** in 19% yield, followed by hydrolysis to give **5** (Scheme 3).

Table 1
Summary of the optimization studies of **1**.

No.	Structure	EP_1 reporter Assay IC_{50} (nM)	cLog P	Clint Rat/human (ml/min/kg)	MDCK (cm/s)
1	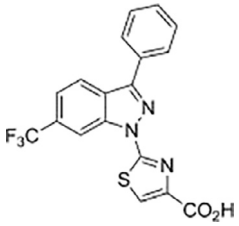	0.6	5.56	186/192	17.8
2	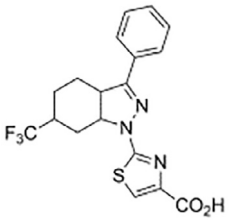	12	4.40	170/102	26.77
3	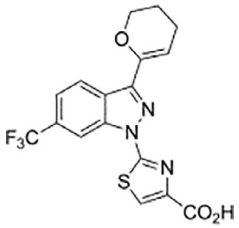	0.7	3.82	232/146	39.02
4	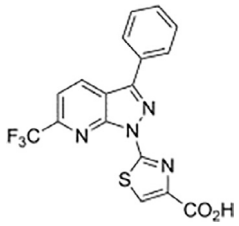	0.3	4.26	94/70	23.47
5	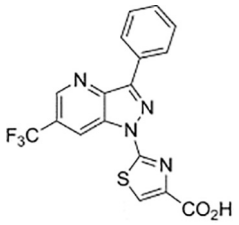	12	4.47		
6	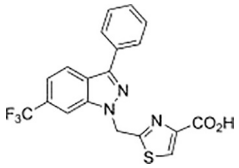	12	5.39	111/48	19.66
7	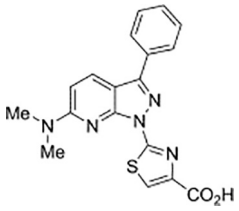	12	3.94		

(*continued on next page*)

Table 1 (*continued*)

No.	Structure	EP_1 reporter Assay IC_{50} (nM)	cLog P	Clint Rat/ human (ml/ min/kg)	MDCK (cm/s)
8	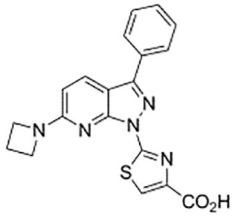	40	3.49		
9	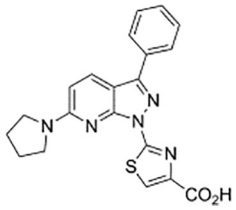	11% inhibition @100 nM	4.05		

(a)

Cpd.	EP_1		EP_2	EP_3	EP_4
	Reporter-gene assay IC_{50} (nM)	Binding assay Ki (nM)			
4	0.3	8.7	>8700	>5000	>2700

(b)

Cpd.	cLogP	C_{max} (μM)	$AUC_{(0-8)}$ (μM/L•h)	Protein Binding	F (%)
1	5.56	5.34	9.27	99.95	31%
4	4.26	2.62	5.71	97.40	26%

(c)

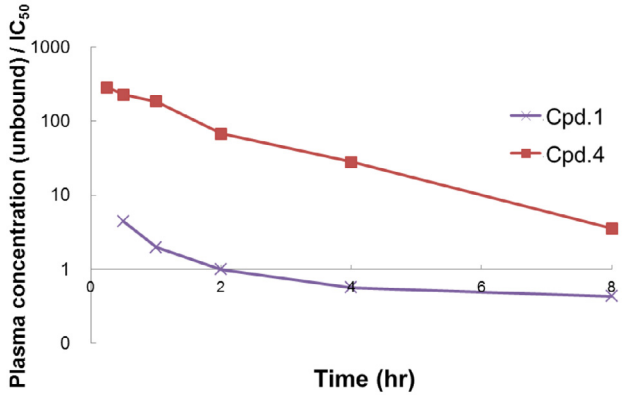

Fig. 2. (a) Selectivity of EP receptor of **1** and **4**; (b) *in vitro* ADME profile of **4**, F (%): bioavailability; (c) Relative ratio of the plasma unbound concentration to the *in vitro* IC_{50} of **4** (pharmacokinetics (PK): rat, p.o., 10 mg/kg, IC_{50}: reporter-gene assay).

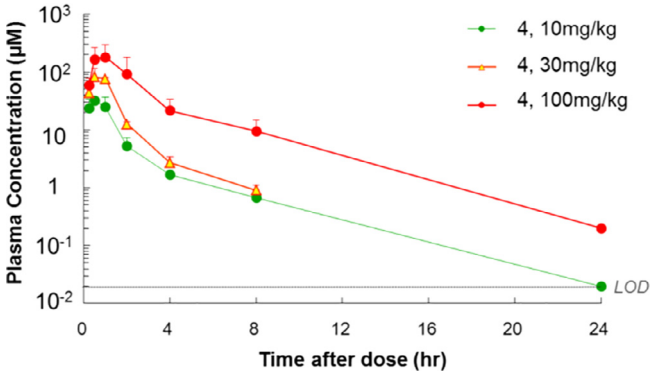

Fig. 3. The pharmacokinetics of **4** following oral administration.

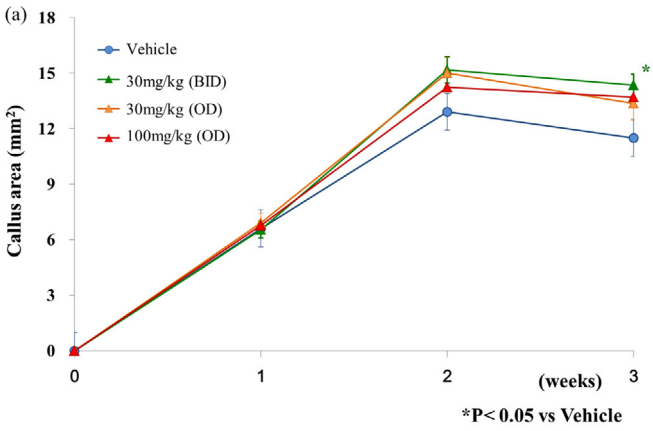

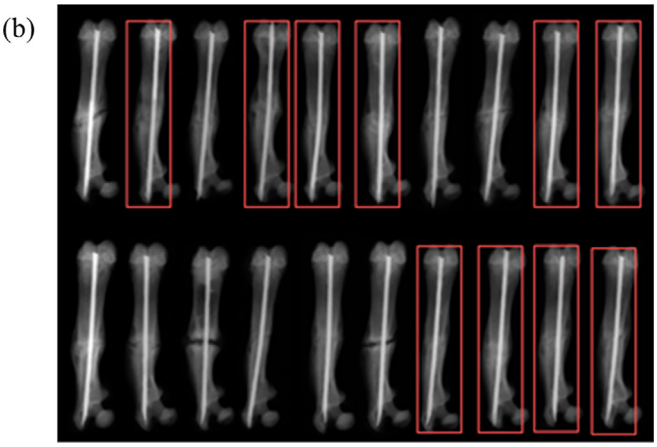

Fig. 4. (a) Time course of thickening in the callus area; (b) Photos of bone following the administration of 100 mg/kg OD.

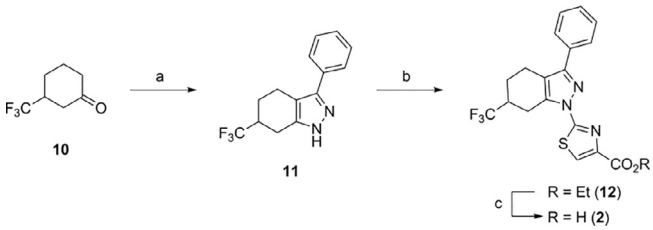

Scheme 1. Reagents and conditions: (a) LHMDS, PhCOCl, THF, rt, then $(NH_2)_2$-H_2O, rt, (11%); (b) ethyl 2-bromothiazole-4-carboxylate, (1*S*,2*S*)-N^1,N^2-dimethylcyclohexane-1,2-diamine, CuI, K_3PO_4, 185 °C (41%); (c) 5 M $NaOH_{(aq)}$, EtOH, rt (76%).

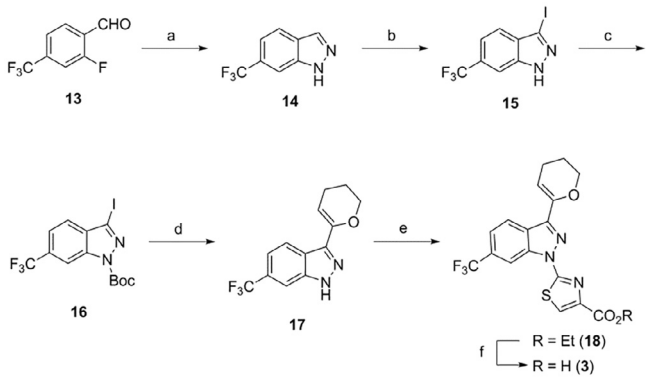

Scheme 2. Reagents and conditions: (a) $MeONH_2$, $(NH_2)_2$-H_2O, THF, 80 °C, (37%); (b) I_2, KOH, DMF (83%); (c) Boc_2O, Et_3N, DMAP, CH_2Cl_2, rt (quant); (d) 3,4-dihydro-2*H*-pyran-6-boronic acid pinacol ester, Pd_2dba_3, K_3PO_4, (*o*-tolyl)$_3$P, toluene, 120 °C (39%); (e) ethyl 2-bromothiazole-4-carboxylate, (1*S*,2*S*)-N^1,N^2-dimethylcyclohexane-1,2-diamine, CuI, K_3PO_4, 185 °C (27%); (f) 5 M $NaOH_{(aq)}$, EtOH, rt (83%).

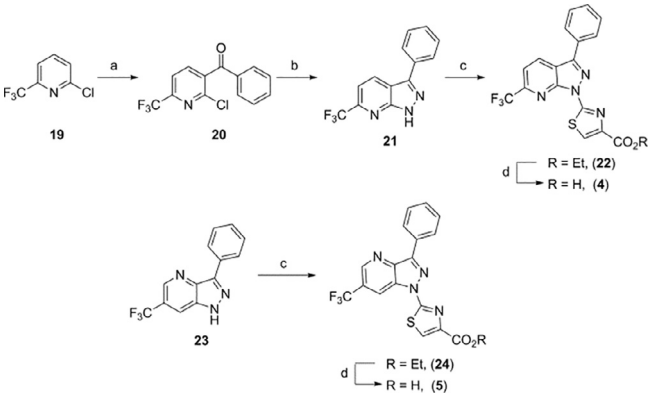

Scheme 3. Reagents and conditions: (a) LDA, THF, −78 °C, then *N*-methoxy-*N*-methylbenzamide (64%); (b) $(NH_2)_2$-H_2O, EtOH, 70 °C, (62%); (c) ethyl 2-bromothiazole-4-carboxylate, (1*S*,2*S*)-N^1,N^2-dimethylcyclo-hexane-1,2-diamine, CuI, K_3PO_4, 185 °C (**22**: 74%. **24**: 19%); (d) 5 M $NaOH_{(aq)}$, EtOH, rt (**4**: 90%, **5**: 88%).

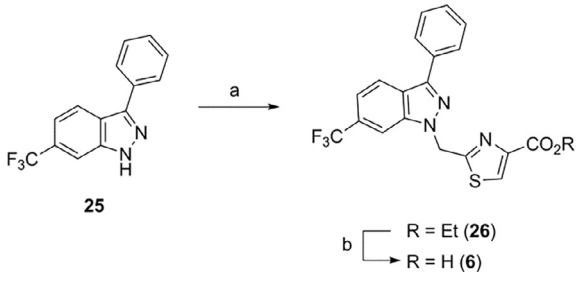

Scheme 4. Reagents and conditions: (a) NaH, DMF, ethyl 2-(bromomethyl) thiazole-4-carboxylate, 0 °C, (14%); (b) 5 M $NaOH_{(aq)}$, EtOH, rt (63%).

N-alkylation of indazole **25** with NaH led to **26**, followed by hydrolysis to give compound **6** (Scheme 4).

Compounds **7–9** were synthesized using the Merck protocol[16] for generation of the 1*H*-pyrazolo[3,4-*b*]pyridine ring to provide **28–30** in 24%, 79% and 6% yield, respectively. Then, Ullmann coupling with **31–33** and subsequent hydrolysis provided compounds **7–9** in 32%, 40% and 30% yield, respectively (Scheme 5).

In conclusion, we identified **4** as the lead compound exhibiting the best EP_1 antagonistic activity, physicochemical properties, and oral pharmacokinetics. A rat bone fracture study with **4** showed that **4** broadened the callus area but did not hasten healing. In future we will disclose our findings from molecular biology mechanistic studies.

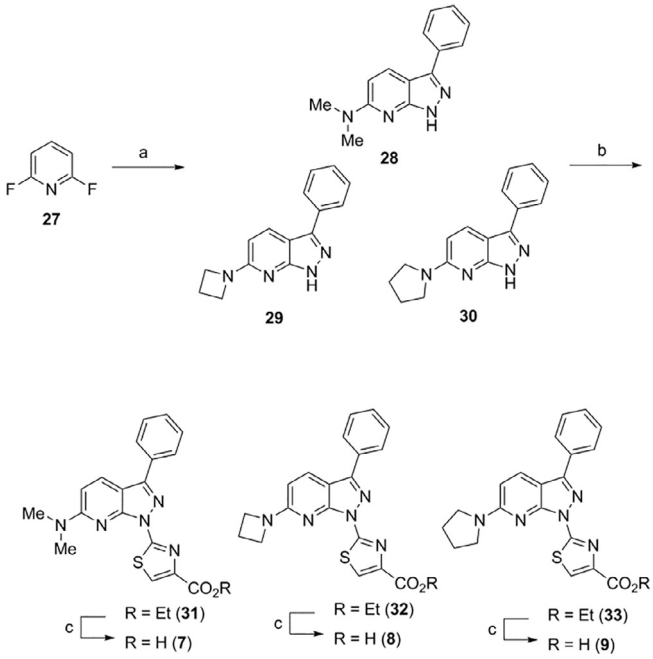

Scheme 5. Reagents and conditions: (a) LDA, THF, −78 °C, then *N*-methoxy-*N*-methylbenzamide, then dimethyl amine/azetidine/pyrrolidine, $(NH_2)_2$-H_2O, THF, rt, (**28**: 24%, **29**: 79%, **30**: 6%); (b) ethyl 2-bromothiazole-4-carboxylate, (1*S*,2*S*)-N^1,N^2-dimethylcyclo-hexane-1,2-diamine, CuI, K_3PO_4, 185 °C (**31**: 51%, **32**: 51%, **33**: 43%); (c) 5 M $NaOH_{(aq)}$, EtOH, rt (**7**: 32%, **8**: 40%, **9**: 30%).

Acknowledgement

The authors thank Rika Komatsu and Sachiko Amishiro for analytical data, and Yoko Miyata for purification support.

A. Supplementary data

Supplementary data associated with this article can be found, in the online version, at http://dx.doi.org/10.1016/j.bmcl.2018.06.022.

References

1. Smyth EM, Grosser T, Wang M, Yu Y, FitzGerald GA. *J Lipid Res.* 2009;50:S423.
2. Breyer RM, Bagdassarian CK, Myers SA, Breyer MD. *Annu Rev Pharmacol Toxicol.* 2001;41:661.
3. Ikeda M, Kawatani M, Maruyama T, Ishihama H. *Biomed Res.* 2006;27:49.
4. Yamaguchi O. *Folia Pharmacol.* 2003;121:331.
5. Atobe M, Naganuma K, Kawanishi M, et al. *Bioorg Med Chem Lett.* 2013;23:6064.
6. Atobe M, Naganuma K, Kawanishi M, et al. *Bioorg Med Chem Lett.* 2013;23:6569.
7. Atobe M, Naganuma K, Kawanishi M, et al. *Bioorg Med Chem Lett.* 2014;24:1327.
8. Chapple CR, Abrams P, Andersson KE, et al. *J Urol.* 2014;191:253.
9. https://www.pharmacodia.com/yaodu/html/v1/chemicals/df74c9ff1542f1574271e759b260543f.html. See related papers; Nishigaya Y, Umei K, Saito Y, et al. *Bioorg Med Chem Lett.* 2017;25:4044.
10. Zhang M, Ho H-c, Sheu T-j, et al. *J Bone Miner Res.* 2011;26:132.
11. PK Study: Compounds **1** and **4** were subjected to PK studies in 7 weeks female Sprague–Dawley rats. Test compounds were administered orally to rats (n = 3) at a dose of 10, 30, 100 mg/kg in 10%v/v DMSO, 5%v/v Cremophor EL, 85%v/v D. water (dose volume 5 ml/kg). Blood samples were collected via the subclavian vein at 0.5, 1, 2, 4, 8, and 24 h post dose. Plasma was separated by centrifugation. Plasma compound concentrations were determined using LC-MS/MS.
12. Femoral fracture model: Closed femur fractures were created in 8-week-old Sprague Dawley rats (Charles-River Laboratories, Inc.) were used for this study. Under anesthesia induced by intraperitoneal (ip) injection with sodium pentobarbital (50 mg/kg per ml; Tokyo Chemical Industry Co., Ltd., Tokyo, Japan), a medial parapatellar arthrotomy was made, and the patella was then dislocated laterally. The 1mm hole was made by drill at intercondylar fossa and a 21-gaude needle (Terumo Corporation, Tokyo, Japan) inserted into the length of medullary canal of the femur from the distal end, and a mid-diaphyseal fracture was created via three-point bending with a three-point bending device “EZ Test, EZ-L-1kN” (SHIMADZU, Kyoto,

Japan). This is based on; Bonnarens F, Einhorn TA. *J Orthop Res*. 1984;2:97. Vehicle (0.5% MC, OD), 30 mg/kg (OD) of 4, 30 mg/kg (BID) of 4 and 100 mg/kg (OD) of 4 were administrated via oral for 28 days after the operation. Blood samples were collected via the subclavian vein at 30 min before administration of 4 (trough value) or 1 h after administration of 4 (Tmax) at 1, 2, 3, 7, 14, 21 and 28 days post dose. Plasma was separated by centrifugation. Plasma compound concentrations were determined using LC-MS/MS. Healing of the femur fracture was monitored using radiographs, which were obtained at 0, 7, 14, 21 and 28 days under anesthesia using a NAOMI digital X-ray system (RF system lab, Japan). The area of the outer hard callus was measured by tracing the callus portion with "Image J" image analysis software (https://imagej.nih.gov/ij/:NIH). Statistics; Results are shown as the mean ± SEM. Statistical significance was identified by *t* tests and two-way ANOVA followed by Dunnett's tests; p values of less than .05 were considered significant.

13. Vina D, Olmo E, López-Pérez JL, Feliciano A. *Org Lett.* 2007;9:525.
14. Antilla JC, Baskin JM, Barder TB, Buchwald SL. *J Org Chem.* 2004;69:5578.
15. Mongin F, Tognini A, Cottet F, Schlosser M. *Tetrahedron Lett.* 1998;39:1749.
16. Tucker TJ, Sisko JT, Tynebor RM, et al. *J Med Chem.* 2008;51:6503.